Development of a Natural Product-Based Selective Fluorescent Sensor for Cu^{2+} and DNA/Protein: Insights from Docking, DFT, Cellular Imaging and Anticancer activity

Sourav Pakrashy[a‡], Manik Das[a‡], Sounik Manna[b], Sujata Maiti Choudhury[b], Hazeena Shinziya[c], Bhriguram Das[d], Malay Dolai[a,*] and Avijit Kumar Das[c,*]

[a] Department of Chemistry, Prabhat Kumar College, Purba Medinipur 721404, W.B., India.
E-mail-dolaimalay@yahoo.in
[b] Biochemistry, Molecular Endocrinology, and Reproductive Physiology Laboratory, Department of Human Physiology, Vidyasagar University, Midnapore721102, W.B., India.

[c] Department of Chemistry, Christ University, Hosur Road, Bangalore, Karnataka, 560029 India, Email: avijitkumar.das@christuniversity.in

[d] Department of Chemistry, Vidyasagar University, Paschim Medinipur 721102, W. B., India.

‡ *Authors are contributed equally*

Experimental details

1. Materials and Methods

All reagents, chemicals, and necessary solvents are research grade and commercially available and were used as received used in this work hence no need for further purification. The Parkin Elmer Fluorescence Spectrometer FL6500 was used for all of the fluorescence spectroscopic investigations.

2. Stock solution preparation for Fluorescence analysis

The stock solution of the sensor **Seselin** ($c = 1\times10^{-3}$ M) was prepared by dissolving the required amount in methanol. Stock solutions of several cations including Zn(II), Co(II), Fe(III), Na(I), Cu(II), Mn(II), Al(III), Mg(II) and Cr(III) ($c = 1\times10^{-5}$ M) were prepared using triple distilled water by using chloride salt of cations. A sufficient amount of the stock solution of **Seselin** (10^{-3} M) was transferred into a 7:3 (v/v) MeOH – H_2O HEPES buffer (pH= 7.4) medium to achieve the desired concentration of 10^{-5} M for accurate estimation of experimental concentration in total fluorescence measurements. Subsequently, using a micropipette, the necessary amount of cationic stock solutions was added separately to it, and spectral measurements were recorded using the quartz optical cell of 1 cm optical path length. Fluorescence measurements were conducted using 5 nm excitation slit width and 5 nm emission slit width.

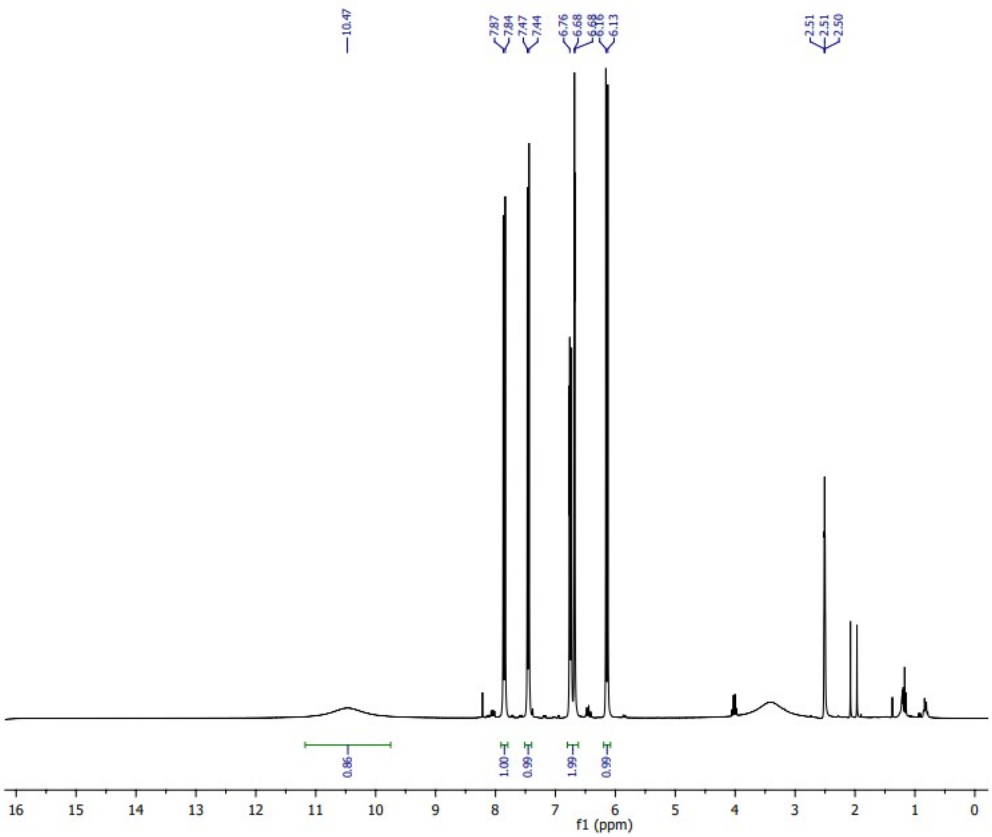

Figure S1. ^{1}H-NMR of **Umbelliferone (3)** in DMSO-d_6.

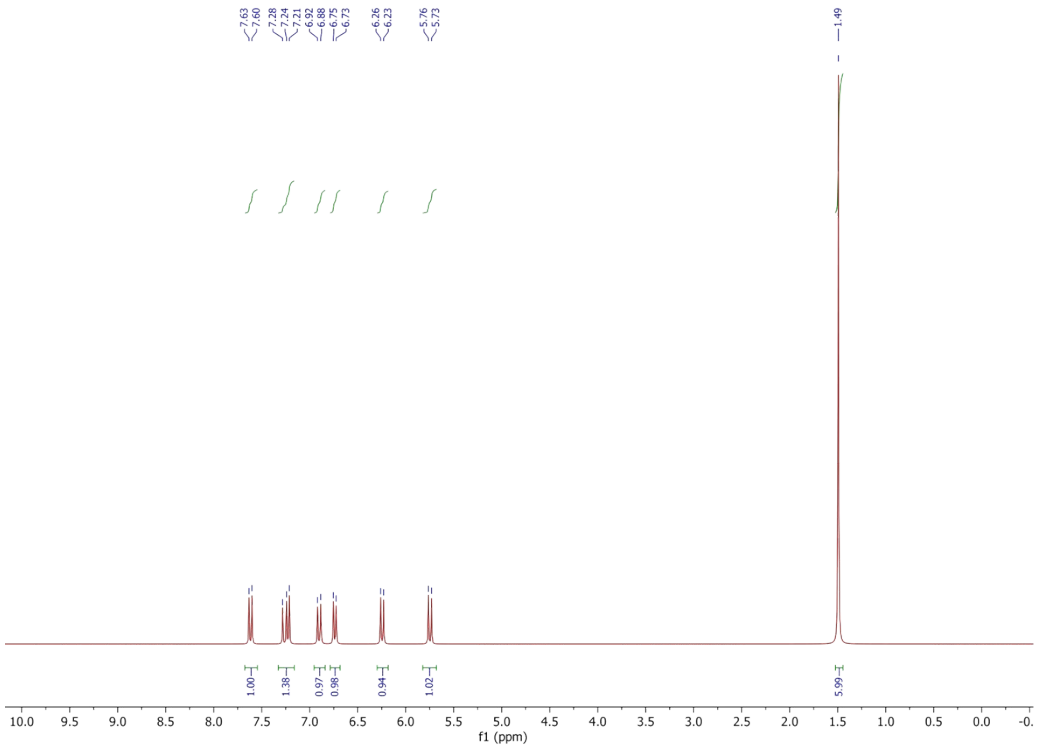

Figure S2.[1]H-NMR of **Seselin**.

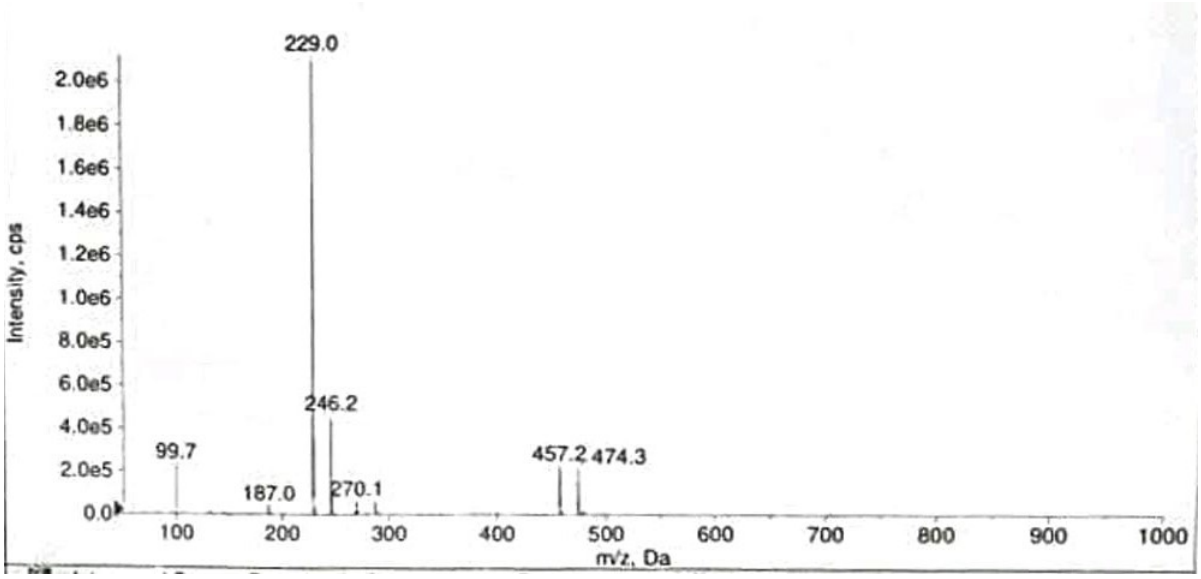

Figure S3. Mass spectra of the probe **Seselin**

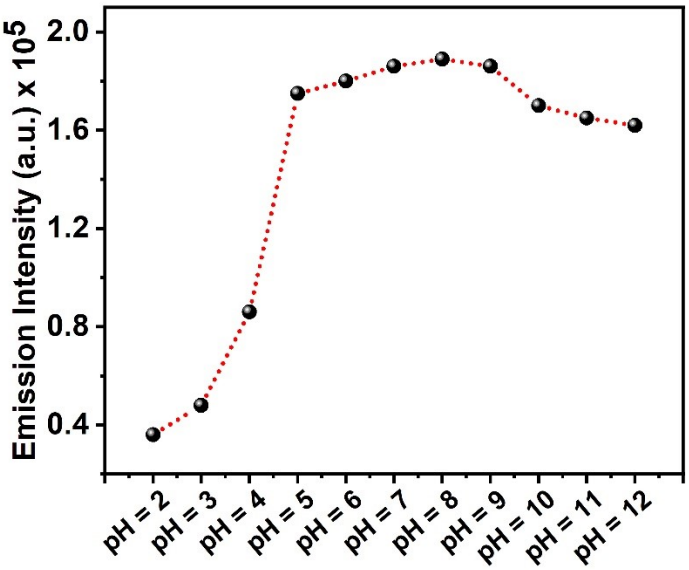

Figure S4: Change of emission intensity of **Seselin** (5×10^{-6} M) in MeOH – H_2O (7:3, v/v) HEPES buffer media at different pH.

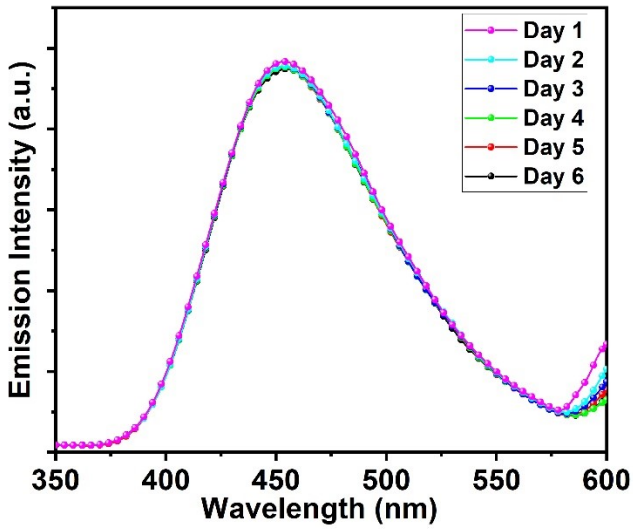

Figure S5: Change of emission intensity of **Seselin** (5×10^{-6} M) as a function of time in MeOH – H_2O (7:3, v/v) HEPES buffer media at pH 7.4.

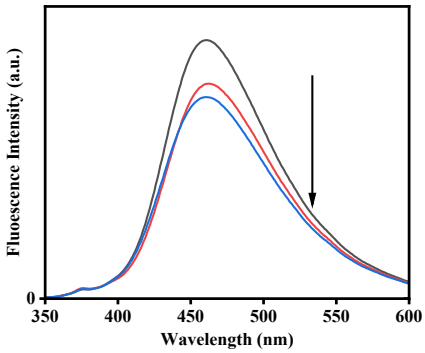

Figure S6. Change of Emission intensity of **SS** (5×10^{-6} M) after incremental addition of Hg^{2+} and Ni^{2+} in MeOH – H_2O (7:3 v/v) HEPES buffer solution at pH 7.4. Red line = Hg^{2+}, blue line= Ni^{2+} and Black = **SS**.

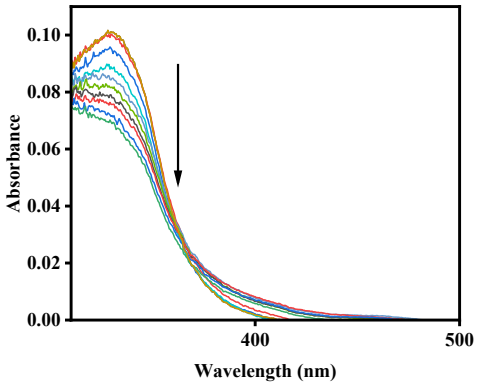

Figure S7. Change in absorbance of **SS** (5×10^{-6} M) after incremental addition of Cu^{2+} (2×10^{-5} M) in MeOH – H_2O (7:3 v/v) HEPES buffer solution at pH 7.4.

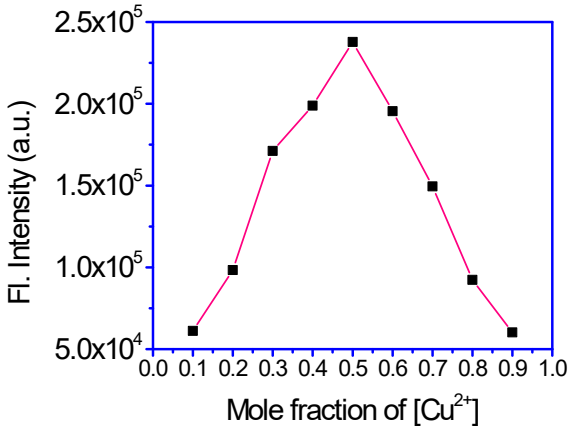

Figure S8. Job's plot diagram of receptor **SS** for Cu^{2+}.

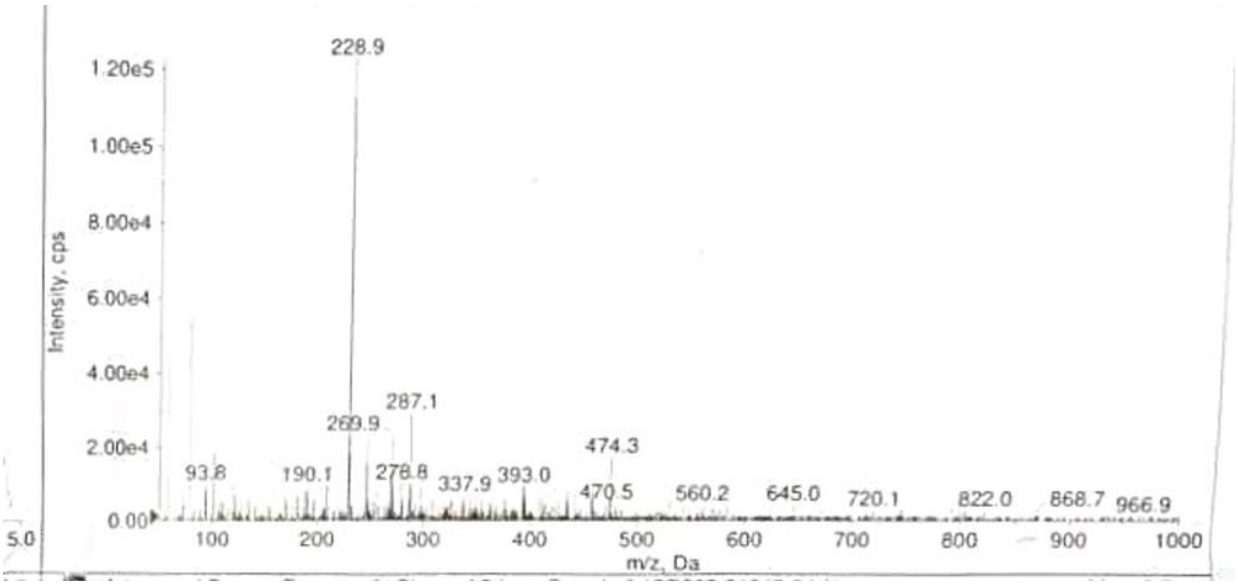

Figure S9. Mass spectra of the probe **seselin** + Cu^{2+}.

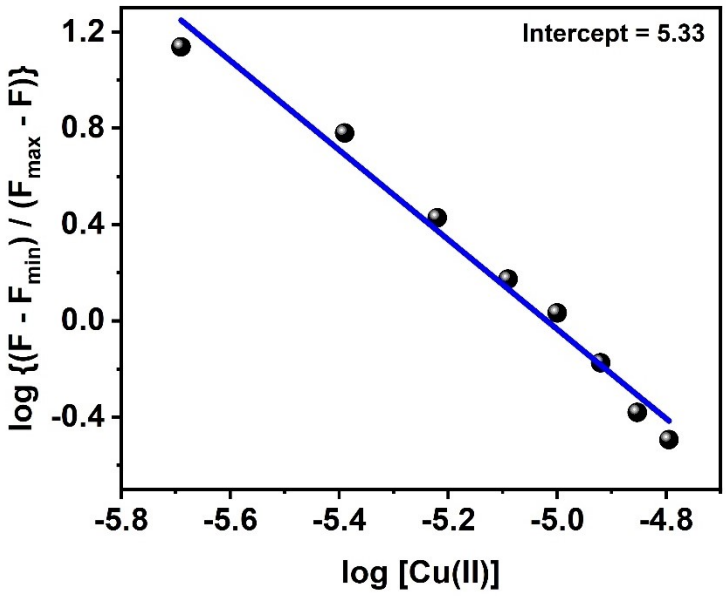

Figure S10. Determination of binding constant of **Seselin** – Cu(II) Complex from the intercept of the plot.

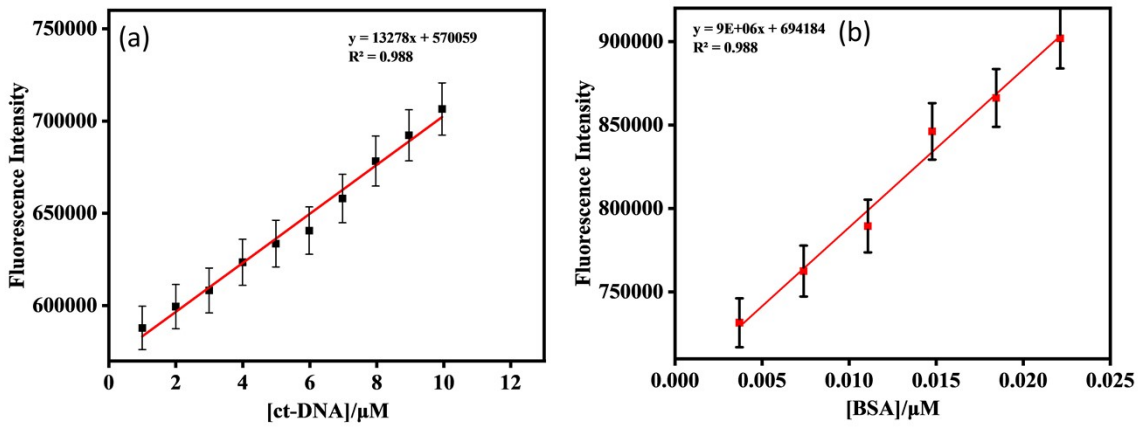

Figure S11. Changes of emission intensity of **Seselin** (c = 2.0 × 10^{-5} M) upon addition of ct DNA (c = 2 mM in base pairs) and BSA (c = 7.4μM).

Binding constant calculation:

The binding constants of **Seselin** with ct DNA and BSA were determined from the fluorometric titration spectra by fitting of the experimental data to the theoretical model in the following equation:[1]

$$\frac{I}{I_0} = 1 + \frac{Q-1}{2}\left(A + xn + 1 - \sqrt{(Q + xn + 1)^2 - 4xn}\right) \quad \text{(Equation 1)}$$

where $Q = I/I_0$ is the minimal emission intensity in the presence of excess ligand; n is the number of independent binding sites per DNA or proteins;

$A = 1/(K_b \times C_{ss})$;

$x = C_{\text{DNA or protein}}/C_{ss}$ is the titration variable

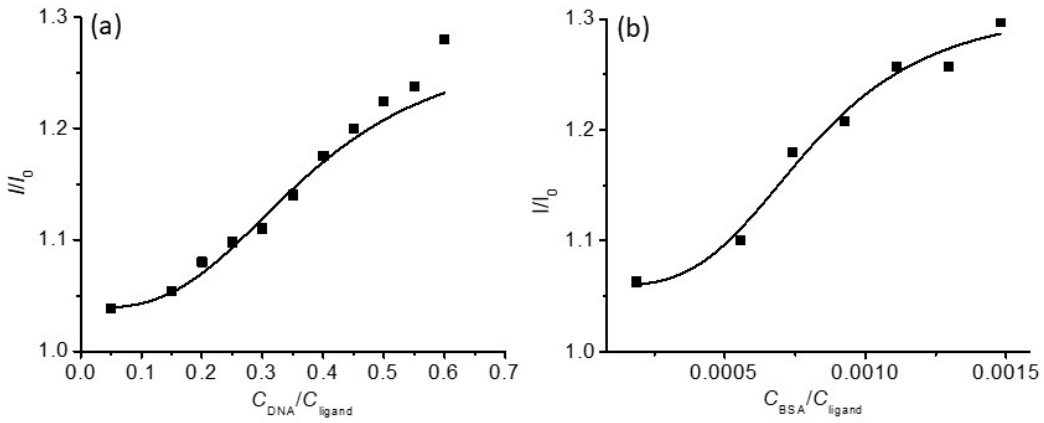

Figure S12. Non-linear fitting curves of binding isotherms from spectrofluorometric titrations of **Seselin** with (a) ct-DNA (b) BSA. Black lines represent the best fits to the theoretical model.

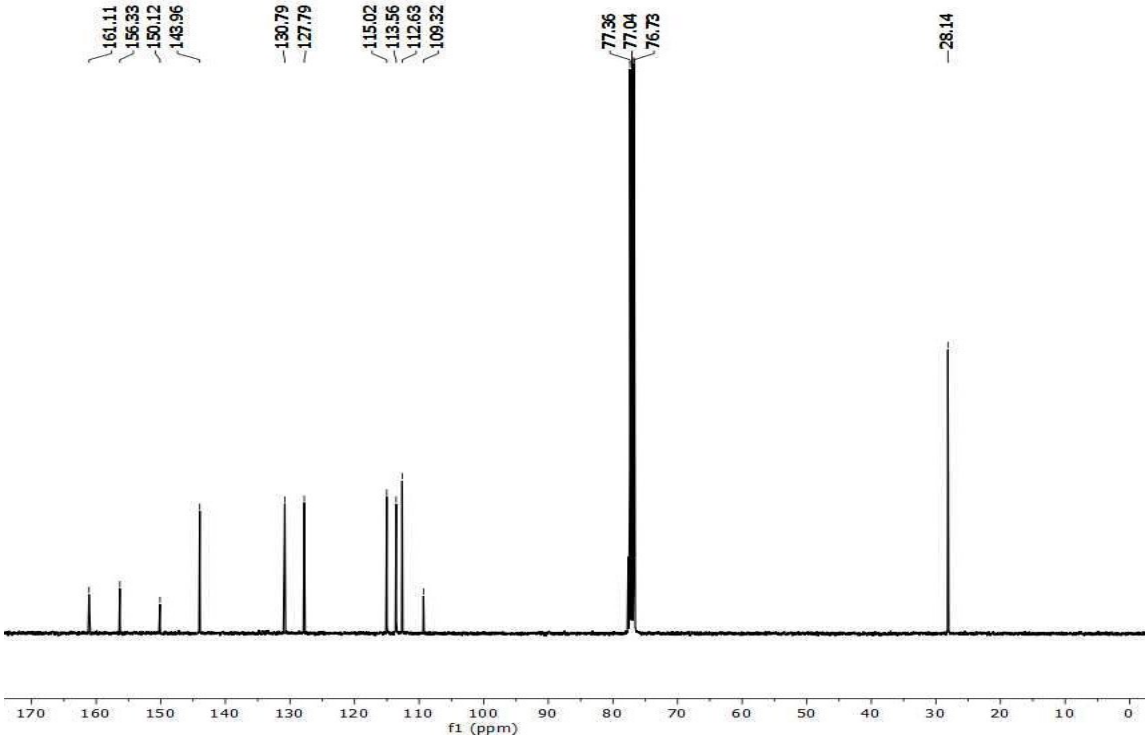

Figure S13. ^{13}C NMR spectra of the probe **Seselin**

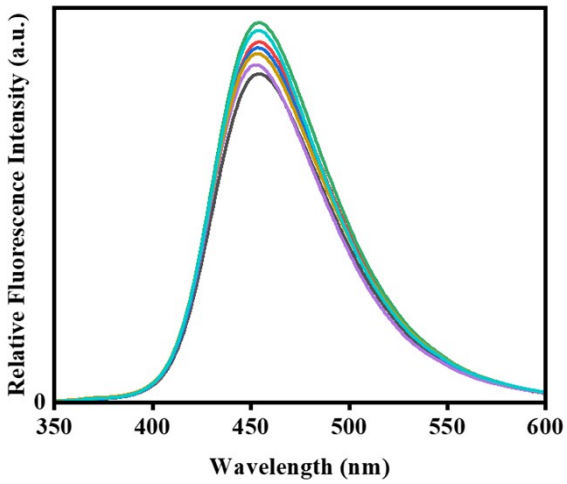

Figure 14. Fluorescence titration of **SS** (c = 2.0 × 10^{-5} M) with isoleucine, phenylalanine, leucine, tryptophan, histidine, methionine, threonine (c = 2 x 10^{-4}) in MeOH:H_2O (7:3 v:v).

3. Evaluation of binding constant

The binding constant K_a of the metal-receptor (Cu^{2+}- **seselin)** complex was determined using the Benesi Hildebrand (B-H) equation separately from absorbance as well as emission titration data.[1-2] Both absorbance and emission titration studies were performed using the stock solution Cu^{2+} (c = 1×10^{-3} mL^{-1}) in aqueous methanol (9:1, v/v) solution.

4. Calculations of the detection limit (LOD)

The detection limit was calculated on the basis of the fluorescence titration. The detection limit (LOD) of the probe **seselin** for Cu^{2+} was determined using the following equation.[3]

$$\text{Detection limit (LOD)} = 3\sigma/k$$

Where σ is the standard deviation of blank measurement, and k is the slope between the fluorescence emission intensity versus metal ion concentration.

5. Computational details

Ground state electronic structure calculations in gas phase of the ligand and complexes have been carried out using DFT[4] method associated with the conductor-like polarizable continuum model (CPCM).[5-7] Becke's hybrid function[8] with the Lee-Yang-Parr (LYP) correlation function[9] was used for the study. The absorbance spectral properties in DMSO medium for **seselin** and **Cu(II)-seselin**, were calculated by time-dependent density functional theory (TDDFT)[10]

associated with the conductor-like polarizable continuum model and we computed the lowest 40 singlet – singlet transition.

For H atoms we used 6-31+(g) basis set; for C, N, O, and Cu atoms we employed LanL2DZ as basis set for all the calculations. The calculated electron-density plots for frontier molecular orbitals were prepared by using Gauss View 5.1 software. All the calculations were performed with the Gaussian 09W software package.[11] Gauss Sum 2.1 program[12] was used to calculate the molecular orbital contributions from groups or atoms.

6. Molecular Docking

The molecular docking methods are conducted according to our previously published papers.[13-15] The bio-macromolecules proteins and DNAs are prepared in UCSF Chimera and Autodock Tools software respectively. For docking purposes Autodock Vina for visualization, UCSF Chimera and Discovery Studio are used.

7. Materials and Methods for bio-imaging

Histopaque 1077, Tetrazolium salt 3-(4, 5-dimethylthiazol-2-yl)-2S-diphenyltetrazolium bromide (MTT), Penicillin and streptomycin, 2',7'-dichlorodihydro fluorescein diacetate (H_2DCFDA), sulfosalicylic acid, Ellman's Reagent (DTNB), 2-vinyl pyridine were purchased from Sigma Aldrich Co, LLC, US. Fetal bovine serum (FBS) and Dulbecco's Modified Eagle Medium (DMEM) were purchased from GIBCO.

Cells viability assay

The biological studies were conducted under aqueous buffered conditions (HEPES, pH 7.4), where methanol acts primarily as a co-solvent (30%) and is not retained in the intracellular environment Seselin (SS) was prepared to be adequately soluble in a MeOH–H_2O (7:3, v/v) mixture buffered with HEPES (10 mM, pH 7.4), ensuring compatibility with cellular environments and enabling efficient intracellular uptake during cytotoxicity assays and bioimaging. MCF-7 cell line was obtained from ABGENEX Private Limited, E-5, KIIT Rd, Infocity, Bhubaneswar, OADISHA 751024, India. Cells were cultured in DMEM and maintained [10% FBS, penicillin (100 U ml-1), and streptomycin (10 mg/mL)] in a humidified atmosphere of 5% CO_2 at 37°C. The cells viability study of seselin against HCT116 cells was performed by tetrazolium salt 3-(4, 5-dimethylthiazol-2-yl)-2S-diphenyltetrazolium bromide

(MTT) assay.[12] Initially, cells (1×10^6 cells/well) were seeded in 96 well-platesand cultured for 72 h. After achieving 80% confluency, cells were exposed to various concentrations of **seselin**, and cells were further cultured for another 24 h in a Co_2 incubator at 37°C. then, DMEM media was removed and cells were washed three times with fresh PBS (pH 7.4). after that, 10 µLof freshly prepared MTT solution (5 mg/mL) was added into each well followed by 3 h incubation at 37°C. after the formation of formazan crystals, 0.1% DMSO was added into each well and allowed to completely dissolve of that formazan crystals. Finally, the absorbance was taken by an ELISA analyzer (Bio-Rad, Model 680) at 540 nm. The 50% inhibitory concentration (IC_{50}) values were analyzed. Cell viability studies of seselin were also performed at different time points (24h, 48h, and 72h) using the same method at their respective IC_{50} doses. The calculation of the percentage of cell viability was performed using the below formula.

$$Cell\ viability\ (\%) = \frac{OD\ of\ sample}{OD\ of\ control} \times 100$$

Isolation and culture of human lymphocyte cell (HLCs)

Around 4 ml of blood was layered onto an equal volume of Histopaque 1077 (Sigma-Aldrich Co. LLC, US) and centrifuged at 2000 rpm for 30 minutes at room temperature. Blood samples of 5 ml were collected from healthy young volunteers following the Hudson and Hay protocol.[16] The lymphocyte layer formed at the top was carefully transferred to a new tube and washed three times with phosphate-buffered solution (pH 7.4). The human lymphocyte cells (HLCs) obtained were then resuspended in RPMI medium supplemented with 10% FBS and incubated for 24 hours at 37°C in a CO_2 incubator with 95% humidity and 5% CO_2. This prepared the HLCs for the cytotoxicity test.

Cell cytotoxicity study

The cytotoxicity of a ligand was assessed using the MTT assay on MCF-7 human breast cancer cells and human lymphocyte cells (HLCs). Cells were seeded in 96-well plates and treated with varying doses of seselin (10-100 µg/ml) for 24 hours in a 37°C, 5% CO_2 environment. After treatment, the cells were washed and incubated with MTT solution, followed by DMSO to dissolve the formazan crystals formed by viable cells. The absorbance at 540 nm was measured using an ELISA analyzer to determine cell viability. The results were expressed as the mean ± SEM from three independent experiments.

Cell imaging study

MCF-7 cells at sub-confluent levels were cultured in DMEM for 24 hours in a CO_2 incubator. seselin was then added to the cells at its IC50 concentration. After incubation, fluorescence images of the MCF-7 cells were captured at 40X magnification using a fluorescence microscope (ZEISS, Germany). Additionally, the cells were treated with a 10 µM solution of Cu^{2+} for one hour, and fluorescence images were taken with excitation wavelengths of 582 and 581 nm for the MCF-7 cells pre-incubated with seselin at the IC_{50} concentration.[17]

Table S1 Comparison table of natural product based fluorescence sensor for Cu^{2+} ion

Sl. No.	**Probe structure**	**Synthetic steps**	**Ex, em**	**LOD**	**Applicability (cell imaging)**	**References**
1	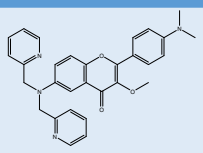	5	390, 510	100 nM	HUVECs	*Sensors and Actuators B: Chemical* *229, 2016, 131-137*
2	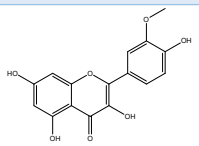 isorhamnetin-ß-CD	1	390, 557	1.7×10^{-8} M	NO	*Chinese Journal of Analytical Chemistry, 2019, 47(6): e19059–e19065*
3	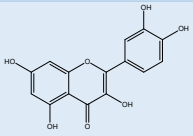	NA	390, 546	1.0×10^{-7} M	NO	*Anal. Methods,* ***2015****, 7: 4546–4551*
4	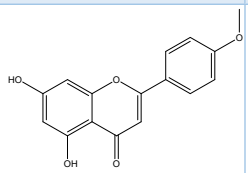	NA	290, 471	1.0 x 10^{-6} M	no	*Sens. Actuators B,* ***2015****, 221: 75–80*

5	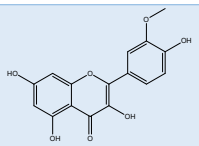	NA	390, 542	4.0×10^{-9} M	NO	*Sens. Actuators B,* ***2016****, 236: 386–391*
6	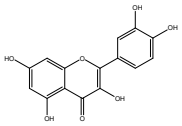	1	390, 553	2.3×10^{-8} M	NO	*RSC Adv., 2018, 8, 37828*
7	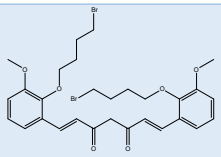	1	420, 562	2.54×10^{-6} M	MCF-7 cells	*Sensors and Actuators B: Chemical* *230, 2016, 684-689*
8	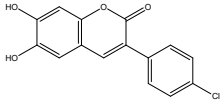	2	366, 456	1.47 nM	NO	*Turk J Chem (2020) 44: 1148 – 1163*
9	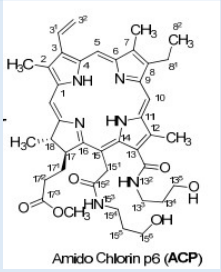	2	412, 668	7.5×10^{-8} M	NO	*Molecules 2016, 21, 107;*
10	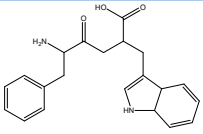	nd	280, 350	10 nM	Hela cell	*ACS Omega 2019, 4, 793-800*
11	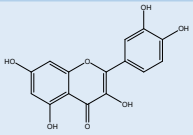 Qc-F127 nano-micelles	1	N D, 535	1.0×10^{-8} M	Hela cells	*Journal of Photochemistry and Photobiology A: Chemistry* *362 2018, 14-20*
12	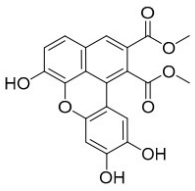	NIL	366, 543	0.574 µM	NO	*Int. J. Mol. Sci.* ***2020****, 21, 6933*

13	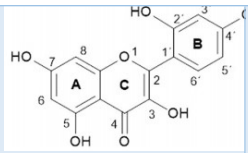 Morrinmagnetic nanoparticles.	3	417, 500	7.5 nM	no	*Sensors and Actuators B 233 (2016) 459–468*
14	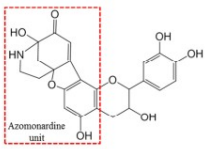 C-DA	1	420, 464	3.0 nM	NO	*Dyes and Pigments* *155, 2018, s 100-106*
15	histidine-derived, biodynamer	1	310, 525	1.56 μM	The A549 cells	*DOI:10.1039/D4LP00126E*
16	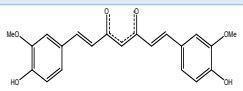	1	420, 507	1.431 ng	NO	*New J. Chem., 2015,39, 7086-7096*
17	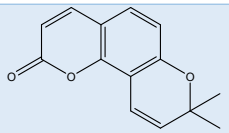	2	**330, 453**	**6.97×10^{-8} M**	**Yes (MCF-7 and HLCs cells)**	**This work**

References:

1. Benesi HA, Hildebrand JH (1949) A Spectrophotometric Investigation of the Interaction of Iodine with Aromatic Hydrocarbons. J Am Chem Soc 71:2703–2707. https://doi.org/10.1021/ja01176a030
2. Banerjee R, Sinha R, Purkayastha P (2019) β-Cyclodextrin Encapsulated Coumarin 6 on Graphene Oxide Nanosheets: Impact on Ground-State Electron Transfer and Excited-State Energy Transfer. ACS Omega 4:16153–16158. https://doi.org/10.1021/acsomega.9b02335
3. Das GC, Das B, Saha U, et al (2024) The crystal structures of Imine-Enamine 'tautomerism' in solid state and "turn on" sensing for Zn^{2+}: spectroscopy, DFT and cell imaging studies. Inorganica Chim Acta 122404. https://doi.org/https://doi.org/10.1016/j.ica.2024.122404
4. Parr RG (1980) Density Functional Theory of Atoms and Molecules BT - Horizons of Quantum Chemistry. In: Fukui K, Pullman B (eds). Springer Netherlands, Dordrecht, pp 5–15
5. Cossi M, Barone V (2001) Time-dependent density functional theory for molecules in liquid solutions. J Chem Phys 115:4708–4717. https://doi.org/10.1063/1.1394921
6. Cossi M, Rega N, Scalmani G, Barone V (2003) Energies, structures, and electronic properties of molecules in solution with the C-PCM solvation model. J Comput Chem 24:669–681. https://doi.org/https://doi.org/10.1002/jcc.10189

7. Barone V, Cossi M (1998) Quantum Calculation of Molecular Energies and Energy Gradients in Solution by a Conductor Solvent Model. J Phys Chem A 102:1995–2001. https://doi.org/10.1021/jp9716997

8. Becke AD (1993) Density-functional thermochemistry. III. The role of exact exchange. J Chem Phys 98:5648–5652. https://doi.org/10.1063/1.464913

9. Lee C, Yang W, Parr RG (1988) Development of the Colle-Salvetti correlation-energy formula into a functional of the electron density. Phys Rev B 37:785–789. https://doi.org/10.1103/PhysRevB.37.785

10. Casida ME, Jamorski C, Casida KC, Salahub DR (1998) Molecular excitation energies to high-lying bound states from time-dependent density-functional response theory: Characterization and correction of the time-dependent local density approximation ionization threshold. J Chem Phys 108:4439–4449. https://doi.org/10.1063/1.475855

11. Frisch Trucks, G.W., Schlegel, H.B., Scuseria, G.E., Robb, M.A., Cheeseman, J.R., Scalmani, G., Barone, V., Mennucci, B., Petersson, G.A., Nakatsuji, H., Caricato, M., Li, X., Hratchian, H.P., Izmaylov, A.F., Bloino, J., Zheng, G., Sonnenberg, J.L., Wall MJ (2009) Gaussian Inc., 2009,. Gaussian Inc, 2009, Wallingford CT. https://doi.org/10.1007/s11172-018-2377-z

12. O'boyle NM, Tenderholt AL, Langner KM (2008) cclib: A library for package-independent computational chemistry algorithms. J Comput Chem 29:839–845. https://doi.org/https://doi.org/10.1002/jcc.20823

13. Morris GM, Lim-Wilby M (2008) Molecular Docking BT - Molecular Modeling of Proteins. In: Kukol A (ed). Humana Press, Totowa, NJ, pp 365–382

14. Pakrashy S, Mandal PK, Dey SK, et al (2022) Design of a Structurally Novel Multipotent Drug Candidate by the Scaffold Architecture Technique for ACE-II, NSP15, and M(pro) Protein Inhibition: Identification and Isolation of a Natural Product to Prevent the Severity of Future Variants of Covid 19 an. ACS omega 7:33408–33422. https://doi.org/10.1021/acsomega.2c04051

15. Das B, Pakrashy S, Das GC, et al (2022) Fashionable Co-operative Sensing of Bivalent Zn^{2+} and Cd^{2+} in Attendance of OAc^- by Use of Simple Sensor: Exploration of Molecular Logic Gate and Docking Studies. J Fluoresc 32:1263–1277. https://doi.org/10.1007/s10895-022-02980-9

16. Hay FC, Hudson L (1989) Practical Immunology, Leslie Hudson, Frank C Hay. Blackwell Scientific Pub

17. Das B, Murmu KC, Dey SK, et al (2024) Pyrazole appended Schiff base based sensor for Al^{3+} detection: Spectroscopic investigation, real sample analysis and cell imaging studies. Inorg Chem Commun 170:113108. https://doi.org/https://doi.org/10.1016/j.inoche.2024.113108